**Journal of NeuroVirology,** 14: 119–129, 2008

ISSN: 1355-0284 print / 1538-2443 online
DOI: 10.1080/13550280701883857

informa
healthcare

# Furious and paralytic rabies of canine origin: Neuroimaging with virological and cytokine studies

Jiraporn Laothamatas,[1] Supaporn Wacharapluesadee,[2] Boonlert Lumlertdacha,[4] Sumate Ampawong,[4] Vera Tepsumethanon,[4] Shanop Shuangshoti,[3] Patta Phumesin,[2] Sawwanee Asavaphatiboon,[1] Ladawan Worapruekjaru,[1] Yingyos Avihingsanon,[2] Nipan Israsena,[2] Monique Lafon,[5] Henry Wilde,[2] and Thiravat Hemachudha[2]

*[1]Department of Radiology, Ramathibodi Hospital, Mahidol University, Bangkok, Thailand; Departments of [2]Medicine and [3]Pathology, Chulalongkorn University Hospital, Bangkok, Thailand; [4]Queen Saovabha Memorial Institute, Thai Red Cross Society, Bangkok, Thailand; [5]Institute Pasteur, Paris, France*

**Furious and paralytic rabies differ in clinical manifestations and survival periods. The authors studied magnetic resonance imaging (MRI) and cytokine and virus distribution in rabies-infected dogs of both clinical types. MRI examination of the brain and upper spinal cord was performed in two furious and two paralytic dogs during the early clinical stage. Rabies viral nucleoprotein RNA and 18 cytokine mRNAs at 12 different brain regions were studied. Rabies viral RNA was examined in four furious and four paralytic dogs during the early stage, and in one each during the late stage. Cytokine mRNAs were examined in two furious and two paralytic dogs during the early stage and in one each during the late stage. Larger quantities of rabies viral RNA were found in the brains of furious than in paralytic dogs. Interleukin-1$\beta$ and interferon-$\gamma$ mRNAs were found exclusively in the brains of paralytic dogs during the early stage. Abnormal hypersignal T2 changes were found at hippocampus, hypothalamus, brainstem, and spinal cord of paralytic dogs. More widespread changes of less intensity were seen in furious dog brains. During the late stage of infection, brains from furious and paralytic rabid dogs were similarly infected and there were less detectable cytokine mRNAs. These results suggest that the early stage of furious dog rabies is characterized by a moderate inflammation (as indicated by MRI lesions and brain cytokine detection) and a severe virus neuroinvasiveness. Paralytic rabies is characterized by delayed viral neuroinvasion and a more intense inflammation than furious rabies. Dogs may be a good model for study of the host inflammatory responses that may modulate rabies virus neuroinvasiveness.** *Journal of NeuroVirology* (2008) **14,** 119–129.

**Keywords:** rabies; pathogenesis; magnetic resonance imaging; cytokines

Address correspondence to Thiravat Hemachudha, MD, Molecular Biology Laboratory for Neurological Diseases, Department of Medicine (Neurology), Faculty of Medicine, Chulalongkorn University Hospital, Rama 4 Road, Bangkok 10330, Thailand. E-mail: thcu@usa.net; fmedthm@gmail.com

This work has been supported in part by grants from the National Science and Technology Development Agency, Thailand, and Advanced Diagnostic Imaging and Image-Guided Minimal Invasive Therapy Center (AIMC), Ramathibodi Hospital.

*Authors' contributions:* JL performed the MRI examination, designed the cradle for dogs for MRI examination and MR protocol for the dog study, and analyzed and interpreted data and was involved in drafting the manuscript. SW developed the protocol for rabies virus and cytokine RNA quantification and analyzed the RNA data and was involved in drafting the manuscript. BL examined the rabid dogs, collected specimens for laboratory confirmation, and developed the cradle for dogs for MR examination. He also cared for dogs during the quarantine period and during the neuroimaging examination. SAm, VT, and SS also took care of the dogs during the quarantine period and during the neuroimaging examination of the animals. PP did the laboratory work in diagnosing rabies and in quantification of rabies virus and cytokine RNA. SAs and LW participated in the designing of the MR protocol and MR examination and analyzing the data. YA and NI were involved in developing cytokine quantification protocol and analysis of the data and in drafting manuscript. ML suggested design, analyzed and interpreted the data, and critically reviewed the manuscript. HW analyzed the data and reviewed the manuscript. TH designed the whole study, confirmed diagnosis, and participated in analyzing and interpreting the data and writing the manuscript. All authors read and approved the final manuscript.

Received 6 August 2007; revised 4 October 2007; accepted 27 November 2007.

## Background

Rabies is caused by a neurotropic RNA virus of genotype 1 in the family *Rhabdoviridae*, genus *Lyssavirus.* Most human deaths are attributable to bites inflicted by rabies infected dogs and wounds contaminated with rabies virus-containing saliva. Once the rabies virus gains access to nerve endings, it travels to the central nervous system (CNS) via retrograde axoplasmic transport and disseminates rapidly throughout the CNS. Two distinct clinical forms, furious and paralytic, are recognized in humans and dogs (Hemachudha, 1994; Hemachudha *et al*, 2002).

In Thailand, we have experience only with the dog strain and no case associated with bat exposure has been recognized (Lumlertdacha *et al*, 2005). Viruses identified in other species, such as cats and wildlife, originate from the dog variant (Denduangboripant *et al*, 2005; Lumlertdacha *et al*, 2006). Only few nucleotide differences in rabies genes were observed between viruses associated with furious and paralytic dogs and humans (Hemachudha *et al*, 2003b; Khawplod *et al*, 2006). The observation that a single Thai dog transmitted furious rabies to one patient and paralytic rabies to another does not support the role of strain differences in determining clinical diversities (Hemachudha *et al*, 2002).

Furious patients tend to die faster (average 5.7 days compared to 11 days in paralytic rabies). Several recent clinical, electrophysiological, and neuropathological findings suggested possible mechanisms for the two clinical forms. Dysfunction of peripheral nerves, not the anterior horn cells, is responsible for clinical weakness in paralytic rabies (Hemachudha *et al*, 2005; Mitrabhakdi *et al*, 2005; Sheikh *et al*, 2005). Despite evidence of anterior horn cell dysfunction in furious rabies, this is not associated with demonstrable weakness (Mitrabhakdi *et al*, 2005). Clinical symptoms of furious rabies are indicative of limbic dysfunctions. These are missing or not prominent in paralytic rabies. Magnetic resonance imaging (MRI), performed during early and late stages of the disease in humans, did not show differences between the two clinical forms (Laothamatas *et al*, 2003; Pleasure and Fischbein, 2000).

The origin of paralytic rabies remains enigmatic. It has been proposed that paralytic rabies could result from lower viral loads in the brain related to longer survival periods and lack of brain symptoms. However, a comparable degree of rabies virus antigen was confined to brainstem, thalami, and basal ganglia in furious as well as in paralytic rabies patients who survived 7 days or less (Tirawatnpong *et al*, 1989). There has been speculation regarding differences in immune responses in human furious and paralytic rabies. However, only peripheral markers, such as measures of cytokines in blood or cerebrospinal fluid (CSF) or immune capacities of circulating cells were assayed in humans. Immune-accelerated death has been hypothesized in furious rabies to explain the rapid fatal course. Six of nine patients who had cellular immunity to rabies virus, determined by lymphocyte proliferation test, manifested as furious rabies, whereas none of seven who had such a response presented as paralytic rabies (Hemachudha *et al*, 1988). Only 1 of 6 paralytic rabies patients (versus 12 of 22 furious) had elevated soluble interleukin (IL)-2 receptor. IL-6 was elevated in 5 of 22 furious and in 0 of 6 paralytic rabies patients (Hemachudha *et al*, 1993).

To assess whether there were differences in the amount of rabies virus and inflammatory/cytokine responses in the brains of furious and paralytic rabies-infected dogs, we studied rabies viral nucleoprotein (N) RNA at 12 different brain regions in four furious and four paralytic dogs during the early stage, and in one each during the late stage. All of these brain regions of two furious and two paralytic dogs during the early stage, and one each during late stage were also determined for the expression of 18 cytokine mRNAs. MRI of the brains of two furious and two paralytic rabies-infected dogs during their early clinical course was also performed. This was to determine whether such abnormalities were in accord with a specific locus for furious symptoms and whether there was a correlation between MRI abnormalities and virus load or inflammatory/cytokine responses.

## Results

### *Determination of rabies viral RNA at different brain regions*

Rabies viral RNA was detected by real-time polymerase chain reaction (PCR) in 12 different regions of the brains of 10 dogs. Four were furious and four paralytic and showed early signs of disease. One was late paralytic and one late furious. Although the number of subjects was limited and may not be appropriate for accurate statistical analysis, larger quantities of rabies viral RNA could be detected in all parts of the brains of furious dogs than in the brains of paralytic dogs. In paralytic dogs, rabies viral RNA was confined mainly to basal ganglia, caudate nucleus, and thalamus and barely detectable in several parts of the brains (Table 1). Basal ganglia, caudate nucleus, thalamus, as well as midbrain were also more heavily infected regions in furious rabid dogs. This suggests that infection was delayed in paralytic as compared to furious dogs. During the late stage, when the animals were obtunded, all brain regions of both furious and paralytic dogs had large amounts of rabies viral RNA.

### *Determination of cytokine mRNA at different brain regions*

Cytokine mRNAs were detected by reverse transcriptase–PCR (RT-PCR) in several brain regions of early (two furious and two paralytic dogs)

**Table 1** Distribution of rabies viral RNA in CNS of rabid dogs

| | Early | | Late | |
|---|---|---|---|---|
| Brain region | Furious* ($n = 4$) | Paralytic* ($n = 4$) | Furious ($n = 1$) | Paralytic ($n = 1$) |
| Frontal | 6.73 ± 2.68 | 0.48 ± 0.33 | 5.20 | ND** |
| Temporal | 6.69 ± 1.89 | 1.48 ± 0.92 | 5.00 | 7.30 |
| Hippocampus | 6.15 ± 2.03 | 0.95 ± 0.55 | 7.90 | 6.00 |
| Parietal | 6.40 ± 1.85 | 0.88 ± 0.69 | 4.00 | 4.60 |
| Occipital | 7.15 ± 3.73 | 0.13 ± 0.07 | 5.60 | 3.90 |
| Midbrain | 10.92 ± 3.36 | 1.87 ± 1.07 | 16.10 | 6.60 |
| Pons | 3.96 ± 1.14 | 1.51 ± 0.90 | 5.30 | 3.60 |
| Medulla | 7.07 ± 2.55 | 1.64 ± 0.98 | 15.30 | 2.90 |
| Cerebellum | 3.14 ± 1.09 | 0.43 ± 0.24 | 4.20 | 6.30 |
| Thalamus | 11.02 ± 2.78 | 2.66 ± 1.53 | 4.80 | 8.60 |
| Basal ganglia | 8.52 ± 2.04 | 5.74 ± 3.43 | 7.80 | 12.90 |
| Caudate nucleus | 10.59 ± 3.95 | 4.56 ± 2.63 | 9.70 | 13.90 |

*Note.* Viral RNA distribution is given as [(copies/$\mu$g total RNA) $\times 10^8$].
*Expressed as mean ± standard error of the mean.
**Sample not available.

and late (one furious and one paralytic) stage rabid dogs (Table 2). However, cytokines that were detected and considered as significant were fewer and mainly present during the early stage and particularly in paralytic dogs. This may suggest that mRNA expression of cytokines in the rabid brain is a transient event. IL-2 mRNA could not be detected in any brain sample. This has been previously observed in other animal (mouse) models (Baloul *et al*, 2004; Galelli *et al*, 2000). Monocyte chemoattractant protein (MCP)-1 was the only cytokine which was found to have an increased ratio to glyceraldehyde 3-phosphate dehydrogenase (GAPDH) area in a normal control dog brain (data not shown). Other cytokines, in this normal control brain, were either non-detectable or their ratio to GAPDH area was <1.

All cytokine mRNAs, except that of IL-2, were detectable in one or both early paralytic dog brains (Table 2). These included, interferon (IFN)-$\gamma$ (2/2), IL-1$\beta$ (2/2), fibroblast growth factor (FGF) (1/2), granulocyte-macrophage colony-stimulating factor (GM-CSF) (1/2), IL-4 (1/2), IL-5 (1/2), IL-6 (1/2), IL-8 (1/2), IL-10 (1/2), IL-12 (1/2), IL-18 (2/2), toll-like receptor (TLR)-4 (2/2), tumor necrosis factor (TNF)-$\alpha$ (1/2), and transforming growth factor (TGF)-$\beta$ (2/2).

Notable differences during the early stage were that IFN-$\gamma$ and IL-1$\beta$ were present exclusively in paralytic dogs (Table 2). These, as well as GM-CSF, IL-2, -4, -8, -10 were nondetectable in all brain regions of two furious dogs. IL-5 was detectable in only one brain region of one furious dog.

Although the cytokines studied were limited and might not be comparable with DNA microarray, they belong to the innate and adaptive immune responses. Despite limitation in sample size, results suggest that brain cytokine transcription inversely correlates with brain virus infection and that IFN-$\gamma$ and IL-1$\beta$ mRNAs expression in the brain could be a hallmark of paralytic rabies.

*MRI examination*

Because MRI analysis can reliably detect brain regions affected by inflammation such as in Japanese encephalitis (Kalita *et al*, 2003), we analyzed whether there were any differences on MRI between paralytic and furious dogs during the early stage of the disease. Two distinct patterns were found (Figures 1 and 2). In both paralytic dogs, abnormal hypersignal T2 changes of mild to moderate degree were noted at the inferomedial temporal lobes and hippocampi (Figure 1; results of only one dog were shown since both had similar patterns). Moderate to marked degree of changes were noted at the hypothalami, midbrain, pons, medulla, and upper spinal cord. In contrast, only diffuse hypersignal T2 changes involving supratentorial structures, such as cerebrum and cerebellum were demonstrated in two furious dogs (Figure 2; results of one dog were shown since both had similar patterns). Lesions at the temporal lobes, brain stem, and spinal cord were also demonstrated. The signal intensity of MRI abnormalities at all brain regions of furious dogs was not as prominent as that in paralytic cases. No gadolinium-contrast lesions were noted in both forms. We have not performed MRI examination of the whole spinal cord due to technical limitations. We used our own modified coiling system and could include only the upper cervical cord in this study. Lacking such MRI data in the spinal cord precludes us from correlating data derived from MRI, virus, and cytokine studies.

These data indicated that dogs with paralytic rabies, in which cytokine mRNAs were mostly transcribed in the brain, were also the dogs showing the clearest MRI abnormalities.

## Discussion

In this comparative analysis of furious and paralytic rabies in dogs, we demonstrated that the brain was

**Table 2** Semiquantitative analysis of cytokine expression from 12 regions of fresh dog brain tissue*

| Brain region | GAPDH | Cox-2 | FGF | GM-CSF | IFN-g | IL-1B | IL-2 | IL-4 | IL-5 | IL-6 | IL-8 | IL-10 | IL-12 p35 | IL-12 p40 | IL-18 | MCP-1 | TLR-4 | TNF-a | TGF-b | VEGF164 | VEGF 188 | VEGF 206 |
|---|---|---|---|---|---|---|---|---|---|---|---|---|---|---|---|---|---|---|---|---|---|---|
| Early Furious No. 10 | | | | | | | | | | | | | | | | | | | | | | |
| Frontal | 131 | 223 | 0 | 0 | 0 | 0 | 0 | 0 | 0 | 0 | 0 | 0 | 88 | 0 | 0 | 157 | 0 | 0 | 140 | 190 | 0 | 174 |
| Temporal | 255 | 77 | 100 | 0 | 0 | 0 | 0 | 0 | 0 | 0 | 0 | 0 | 167 | 0 | 0 | 118 | 0 | 0 | 149 | 211 | 0 | 174 |
| Hippocampus | 255 | 78 | 79 | 0 | 0 | 0 | 0 | 0 | 0 | 0 | 0 | 0 | 217 | 0 | 0 | 217 | 0 | 143 | 95 | 223 | 0 | 195 |
| Parietal | 255 | 0 | 100 | 0 | 0 | 0 | 0 | 0 | 0 | 0 | 0 | 0 | 108 | 0 | 78 | 211 | 101 | 143 | 95 | 223 | 0 | 197 |
| Occipital | 255 | 62 | 110 | 0 | 0 | 0 | 0 | 0 | 0 | 0 | 0 | 0 | 140 | 0 | 164 | 255 | 190 | 143 | 175 | 240 | 0 | 197 |
| Midbrain | 255 | 59 | 86 | 0 | 0 | 0 | 0 | 0 | 0 | 0 | 0 | 0 | 112 | 0 | 126 | 227 | 190 | 143 | 163 | 233 | 0 | 201 |
| Pons | 149 | 51 | 0 | 0 | 0 | 0 | 0 | 0 | 0 | 0 | 0 | 0 | 138 | 0 | 75 | 217 | 130 | 143 | 143 | 227 | 0 | 201 |
| Medulla | 184 | 48 | 72 | 0 | 0 | 0 | 0 | 0 | 0 | 0 | 0 | 0 | 105 | 0 | 0 | 206 | 0 | 143 | 147 | 233 | 0 | 201 |
| Cerebellum | 255 | 59 | 0 | 0 | 0 | 0 | 0 | 0 | 0 | 0 | 0 | 0 | 97 | 0 | 0 | 148 | 0 | 143 | 94 | 207 | 0 | 144 |
| Thalamus | 255 | 0 | 0 | 0 | 0 | 0 | 0 | 0 | 0 | 0 | 0 | 0 | 80 | 0 | 0 | 98 | 0 | 123 | 0 | 207 | 0 | 174 |
| Basal ganglia | 255 | 0 | 95 | 0 | 0 | 0 | 0 | 0 | 0 | 0 | 0 | 0 | 108 | 0 | 0 | 165 | 0 | 0 | 92 | 211 | 0 | 174 |
| Caudate | 77 | 0 | 0 | 0 | 0 | 0 | 0 | 0 | 0 | 0 | 0 | 0 | 86 | 0 | 0 | 108 | 0 | 0 |  | 249 | 0 | 165 |
| Early Furious No. 8 | | | | | | | | | | | | | | | | | | | | | | |
| Frontal | 141 | 0 | 103 | 0 | 0 | 0 | 0 | 0 | 0 | 0 | 0 | 0 | 127 | 0 | 180 | 127 | 109 | 0 | 0 | 190 | 0 | 174 |
| Temporal | 149 | 0 | 101 | 0 | 0 | 0 | 0 | 0 | 0 | 0 | 0 | 0 | 179 | 0 | 110 | 110 | 117 | 0 | 0 | 211 | 0 | 174 |
| Hippocampus | 178 | 0 | 126 | 0 | 0 | 0 | 0 | 0 | 0 | 108 | 0 | 0 | 170 | 0 | 155 | 215 | 127 | 0 | 133 | 223 | 0 | 195 |
| Parietal | 196 | 0 | 107 | 0 | 0 | 0 | 0 | 0 | 111 | 105 | 0 | 0 | 0 | 0 | 0 | 207 | 134 | 0 | 0 | 223 | 0 | 197 |
| Occipital | 191 | 0 | 115 | 0 | 0 | 0 | 0 | 0 | 0 | 99 | 0 | 0 | 149 | 0 | 167 | 165 | 130 | 115 | 133 | 240 | 0 | 197 |
| Midbrain | 130 | 0 | 127 | 0 | 0 | 0 | 0 | 0 | 0 | 99 | 0 | 0 | 0 | 0 | 187 | 127 | 119 | 0 | 131 | 233 | 0 | 201 |
| Pons | 135 | 0 | 0 | 0 | 0 | 0 | 0 | 0 | 0 | 0 | 0 | 0 | 0 | 0 | 144 | 152 | 0 | 0 | 0 | 227 | 0 | 201 |
| Medulla | 146 | 221 | 0 | 0 | 0 | 0 | 0 | 0 | 0 | 0 | 0 | 0 | 0 | 0 | 175 | 141 | 0 | 0 | 0 | 233 | 0 | 201 |
| Cerebellum | 119 | 0 | 0 | 0 | 0 | 0 | 0 | 0 | 0 | 0 | 0 | 0 | 0 | 0 | 113 | 197 | 0 | 0 | 0 | 207 | 0 | 144 |
| Thalamus | 170 | 0 | 116 | 0 | 0 | 0 | 0 | 0 | 0 | 101 | 0 | 0 | 0 | 0 | 201 | 225 | 134 | 99 | 151 | 207 | 0 | 174 |
| Basal ganglia | 151 | 0 | 118 | 0 | 0 | 0 | 0 | 0 | 0 | 116 | 0 | 0 | 145 | 0 | 119 | 214 | 123 | 0 | 134 | 211 | 0 | 174 |
| Caudate | 120 | 0 | 0 | 0 | 0 | 0 | 0 | 0 | 0 | 165 | 0 | 0 | 145 | 0 | 0 | 153 | 112 | 0 | 0 | 249 | 0 | 165 |
| Early Paralytic No. 7 | | | | | | | | | | | | | | | | | | | | | | |
| Frontal | 157 | 110 | 0 | 0 | 105 | 134 | 0 | 0 | 0 | 0 | 0 | 0 | 0 | 0 | 62 | 122 | 102 | 0 | 0 | 71 | 0 | 0 |
| Temporal | 137 | 111 | 0 | 0 | 110 | 151 | 0 | 0 | 0 | 0 | 0 | 0 | 0 | 0 | 0 | 255 | 106 | 0 | 0 | 70 | 0 | 0 |
| Hippocampus | 184 | 118 | 0 | 0 | 152 | 134 | 0 | 0 | 0 | 0 | 0 | 0 | 0 | 0 | 0 | 104 | 73 | 0 | 99 | 82 | 0 | 0 |
| Parietal | 255 | 99 | 0 | 0 | 0 | 0 | 0 | 0 | 0 | 0 | 0 | 0 | 0 | 0 | 78 | 116 | 0 | 0 | 99 | 145 | 0 | 0 |
| Occipital | 255 | 97 | 0 | 0 | 0 | 0 | 0 | 0 | 0 | 0 | 0 | 0 | 0 | 0 | 0 | 0 | 0 | 0 | 112 | 202 | 0 | 0 |
| Midbrain | 153 | 128 | 0 | 0 | 132 | 0 | 0 | 0 | 0 | 0 | 0 | 0 | 0 | 0 | 123 | 207 | 123 | 0 | 160 | 240 | 0 | 0 |
| Pons | 147 | 95 | 0 | 0 | 127 | 143 | 0 | 0 | 0 | 0 | 0 | 0 | 0 | 0 | 240 | 134 | 106 | 0 | 200 | 255 | 0 | 0 |
| Medulla | 163 | 87 | 0 | 0 | 127 | 130 | 0 | 0 | 0 | 0 | 0 | 0 | 0 | 0 | 200 | 147 | 67 | 0 | 0 | 65 | 0 | 0 |
| Cerebellum | 100 | 86 | 0 | 0 | 164 | 134 | 0 | 0 | 0 | 0 | 0 | 0 | 0 | 0 | 0 | 0 | 0 | 0 | 0 | 65 | 0 | 0 |
| Thalamus | 85 | 72 | 0 | 0 | 0 | 115 | 0 | 0 | 0 | 0 | 0 | 0 | 0 | 0 | 0 | 105 | 84 | 0 | 0 | 70 | 0 | 0 |
| Basal ganglia | 56 | 72 | 0 | 0 | 110 | 124 | 0 | 0 | 0 | 0 | 0 | 0 | 0 | 0 | 64 | 131 | 0 | 0 | 153 | 231 | 0 | 0 |
| Caudate | 56 | 115 | 0 | 0 | 0 | 135 | 0 | 0 | 0 | 0 | 0 | 0 | 0 | 0 | 73 | 86 | 64 | 0 | 110 | 255 | 0 | 0 |
| Early Paralytic No. 32 | | | | | | | | | | | | | | | | | | | | | | |
| Frontal | 167 | 234 | 214 | 189 | 233 | 255 | 0 | 171 | 199 | 251 | 242 | 192 | 210 | 182 | 193 | 245 | 86 | 225 | 140 | 233 | 156 | 170 |
| Temporal | 176 | 213 | 212 | 164 | 124 | 212 | 0 | 87 | 203 | 237 | 222 | 131 | 180 | 178 | 192 | 229 | 79 | 225 | 139 | 237 | 152 | 180 |
| Hippocampus | 197 | 217 | 203 | 218 | 243 | 220 | 0 | 191 | 167 | 252 | 233 | 180 | 226 | 175 | 238 | 229 | 84 | 221 | 150 | 233 | 135 | 185 |
| Parietal | 218 | 225 | 215 | 206 | 94 | 218 | 0 | 173 | 191 | 244 | 232 | 176 | 208 | 139 | 236 | 234 | 0 | 224 | 184 | 227 | 157 | 175 |
| Occipital | 220 | 230 | 216 | 151 | 218 | 195 | 0 | 101 | 209 | 226 | 241 | 157 | 209 | 152 | 226 | 233 | 85 | 208 | 187 | 234 | 147 | 174 |
| Midbrain | 235 | 168 | 207 | 225 | 244 | 107 | 0 | 196 | 132 | 239 | 237 | 244 | 188 | 233 | 233 | 219 | 78 | 179 | 164 | 229 | 125 | 130 |
| Pons | 240 | 140 | 190 | 227 | 199 | 117 | 0 | 194 | 128 | 231 | 213 | 253 | 111 | 224 | 222 | 238 | 0 | 217 | 177 | 225 | 118 | 132 |
| Medulla | 240 | 188 | 222 | 215 | 142 | 120 | 0 | 170 | 125 | 231 | 207 | 223 | 191 | 214 | 224 | 235 | 71 | 215 | 163 | 223 | 141 | 150 |
| Cerebellum | 244 | 204 | 209 | 204 | 123 | 152 | 0 | 173 | 122 | 236 | 188 | 225 | 164 | 116 | 215 | 224 | 0 | 182 | 58 | 226 | 119 | 130 |
| Thalamus | 235 | 201 | 207 | 230 | 219 | 181 | 0 | 203 | 121 | 226 | 149 | 244 | 203 | 139 | 215 | 226 | 66 | 206 | 99 | 223 | 142 | 176 |
| Basal ganglia | 233 | 192 | 225 | 150 | 94 | 226 | 0 | 93 | 130 | 248 | 182 | 165 | 192 | 219 | 219 | 231 | 60 | 231 | 106 | 220 | 147 | 190 |
| Caudate | 242 | 198 | 214 | 117 | 62 | 244 | 0 | 71 | 156 | 251 | 226 | 155 | 205 | 234 | 215 | 236 | 0 | 243 | 101 | 222 | 155 | 200 |

| | | | | | | | | | | | | | | | | | | | | | | |
|---|---|---|---|---|---|---|---|---|---|---|---|---|---|---|---|---|---|---|---|---|---|---|
| Late Furious No. 11 | | | | | | | | | | | | | | | | | | | | | | |
| Frontal | 139 | 0 | 0 | 0 | 0 | 0 | 0 | 0 | 0 | 0 | 0 | 0 | 0 | 0 | 0 | 80 | 0 | 0 | 0 | 132 | 0 | 111 |
| Temporal | 180 | 0 | 0 | 0 | 0 | 0 | 0 | 0 | 0 | 0 | 0 | 0 | 158 | 0 | 106 | 145 | 122 | 0 | 164 | 124 | 0 | 113 |
| Hippocampus | 141 | 0 | 0 | 0 | 0 | 0 | 0 | 0 | 0 | 0 | 0 | 0 | 165 | 0 | 62 | 98 | 128 | 0 | 164 | 135 | 0 | 119 |
| Parietal | 100 | 0 | 0 | 0 | 0 | 0 | 0 | 0 | 0 | 0 | 0 | 0 | 154 | 0 | 0 | 82 | 140 | 0 | 163 | 128 | 0 | 116 |
| Occipital | 211 | 0 | 0 | 0 | 0 | 0 | 0 | 0 | 0 | 0 | 0 | 0 | 154 | 0 | 0 | 125 | 121 | 0 | 170 | 145 | 0 | 120 |
| Midbrain | 245 | 0 | 0 | 0 | 0 | 0 | 0 | 0 | 0 | 0 | 0 | 0 | 167 | 0 | 0 | 88 | 132 | 0 | 0 | 125 | 0 | 115 |
| Pons | 200 | 0 | 0 | 0 | 0 | 0 | 0 | 0 | 0 | 0 | 0 | 0 | 0 | 0 | 0 | 87 | 128 | 0 | 0 | 117 | 0 | 110 |
| Medulla | 233 | 0 | 0 | 0 | 0 | 0 | 0 | 0 | 0 | 0 | 0 | 0 | 0 | 0 | 0 | 151 | 120 | 0 | 162 | 122 | 0 | 108 |
| Cerebellum | 185 | 0 | 0 | 0 | 0 | 0 | 0 | 0 | 0 | 0 | 0 | 0 | 166 | 0 | 0 | 76 | 128 | 0 | 157 | 111 | 0 | 107 |
| Thalamus | 100 | 0 | 0 | 0 | 0 | 0 | 0 | 0 | 0 | 0 | 0 | 0 | 0 | 0 | 0 | 76 | 120 | 0 | 0 | 106 | 0 | 109 |
| Basal ganglia | 200 | 0 | 0 | 0 | 0 | 0 | 0 | 0 | 0 | 0 | 0 | 0 | 156 | 0 | 0 | 87 | 114 | 0 | 137 | 140 | 0 | 117 |
| Caudate | 200 | 0 | 0 | 0 | 0 | 0 | 0 | 0 | 0 | 0 | 0 | 0 | 169 | 0 | 0 | 75 | 129 | 0 | 140 | 127 | 0 | 109 |
| Late Paralytic No. 23 | | | | | | | | | | | | | | | | | | | | | | |
| Frontal | ND | ND | ND | ND | ND | ND | ND | ND | ND | ND | ND | ND | ND | ND | ND | ND | ND | ND | ND | ND | ND | ND |
| Temporal | 255 | 165 | 210 | 0 | 97 | 0 | 0 | 0 | 0 | 116 | 0 | 0 | 90 | 0 | 0 | 144 | 0 | 0 | 0 | 232 | 0 | 127 |
| Hippocampus | 255 | 0 | 191 | 0 | 100 | 100 | 0 | 0 | 0 | 166 | 0 | 0 | 86 | 0 | 0 | 74 | 0 | 0 | 0 | 223 | 0 | 128 |
| Parietal | 119 | 0 | 0 | 0 | 118 | 100 | 0 | 0 | 0 | 158 | 0 | 0 | 60 | 0 | 0 | 97 | 0 | 0 | 0 | 210 | 0 | 122 |
| Occipital | 178 | 0 | 93 | 0 | 102 | 120 | 0 | 0 | 0 | 128 | 0 | 0 | 56 | 0 | 110 | 124 | 126 | 0 | 0 | 255 | 0 | 142 |
| Midbrain | 200 | 0 | 116 | 0 | 133 | 100 | 0 | 0 | 0 | 108 | 0 | 0 | 0 | 0 | 128 | 255 | 219 | 0 | 0 | 255 | 0 | 165 |
| Pons | 255 | 143 | 137 | 0 | 126 | 100 | 0 | 0 | 0 | 121 | 0 | 0 | 60 | 0 | 130 | 207 | 241 | 0 | 0 | 229 | 0 | 142 |
| Medulla | 255 | 134 | 118 | 0 | 221 | 92 | 0 | 0 | 0 | 163 | 0 | 0 | 0 | 0 | 99 | 100 | 140 | 0 | 0 | 178 | 0 | 115 |
| Cerebellum | 223 | 0 | 114 | 0 | 100 | 0 | 0 | 0 | 0 | 80 | 0 | 0 | 90 | 0 | 86 | 55 | 86 | 0 | 0 | 241 | 0 | 170 |
| Thalamus | 117 | 0 | 0 | 0 | 0 | 98 | 0 | 0 | 0 | 0 | 0 | 0 | 0 | 0 | 0 | 0 | 0 | 0 | 0 | 255 | 0 | 150 |
| Basal ganglia | 113 | 0 | 0 | 0 | 80 | 78 | 0 | 0 | 0 | 80 | 0 | 0 | 0 | 0 | 0 | 0 | 0 | 0 | 0 | 255 | 0 | 192 |
| Caudate | 120 | 0 | 0 | 0 | 87 | 0 | 0 | 0 | 0 | 110 | 0 | 0 | 0 | 0 | 0 | 87 | 163 | 0 | 0 | 255 | 0 | 187 |

*The gels were quantified by video image analysis software and the expression rates were calculated as a ratio of cytokine to GAPDH area from the same sample. ND = not done. Zero and numbers in shaded area represent nondetectable cytokines and values considered significant. Unshaded numbers represent values considered detectable.

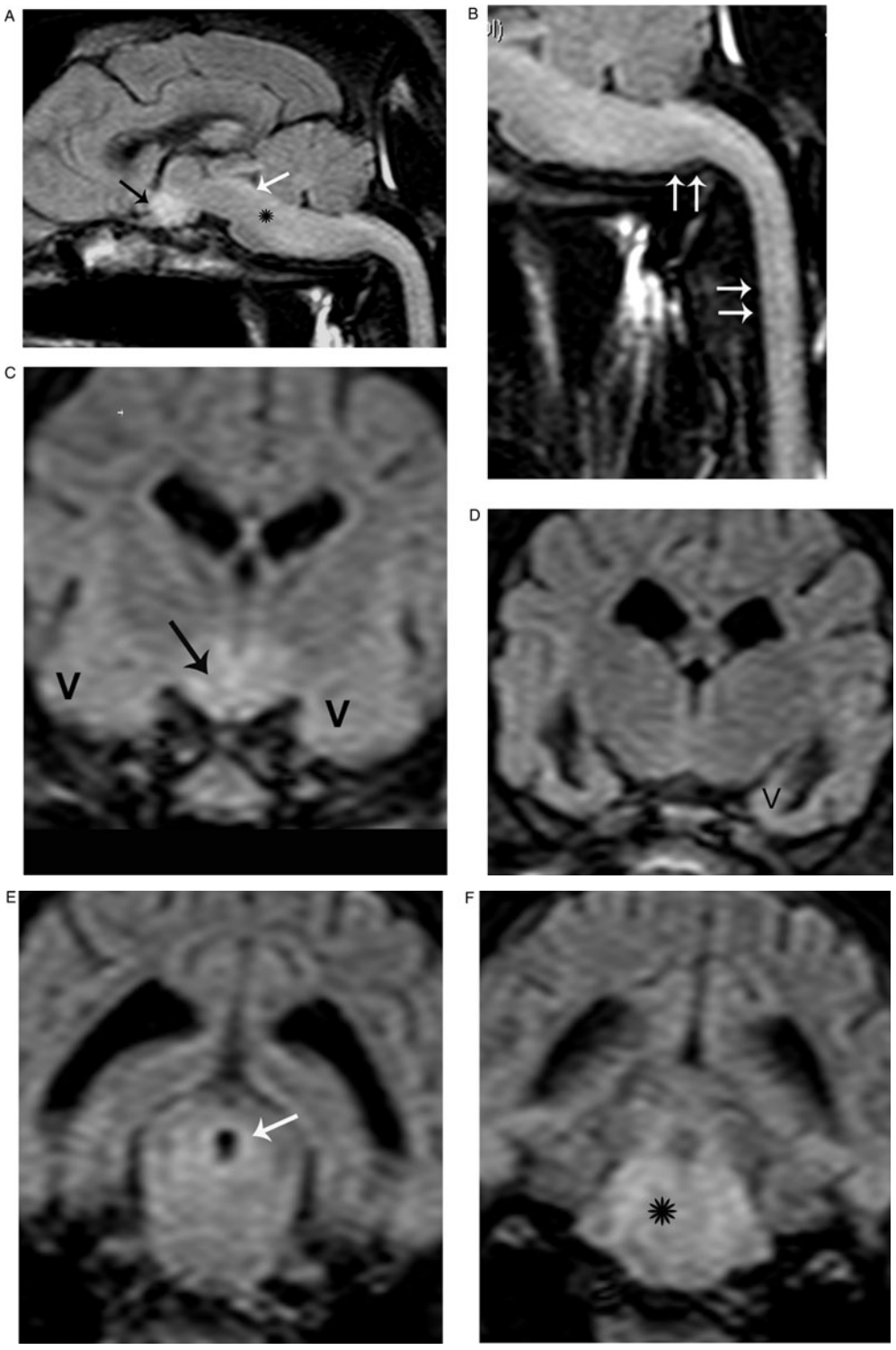


**Figure 1** Sagittal (A, B) and coronal (C to F) T2-weighted FLAIR MR images of a paralytic rabid dog brain reveal moderate to marked abnormal hypersignal T2 changes at the hypothalamus (*black arrow* in A and C), midbrain (*white arrow* in A and E), pons (black asterix in A and F), medulla and upper spinal cord (*double arrows* in B). Less intense hypersignal T2 changes are also observed at the anteroinferomedial temporal lobes (*black V* in C and D). No significant abnormality of the cerebrum is observed.

rapidly colonized by the virus in furious rabies. Yet, only mild MRI changes and weak cytokine transcription could be detected. This was in striking contrast to brains of paralytic rabid dogs, which showed stronger disturbances in MRI signals and in inflammatory cytokine responses with slower neuroinvasiveness. These distinctions could not be observed in the later stage of the disease.

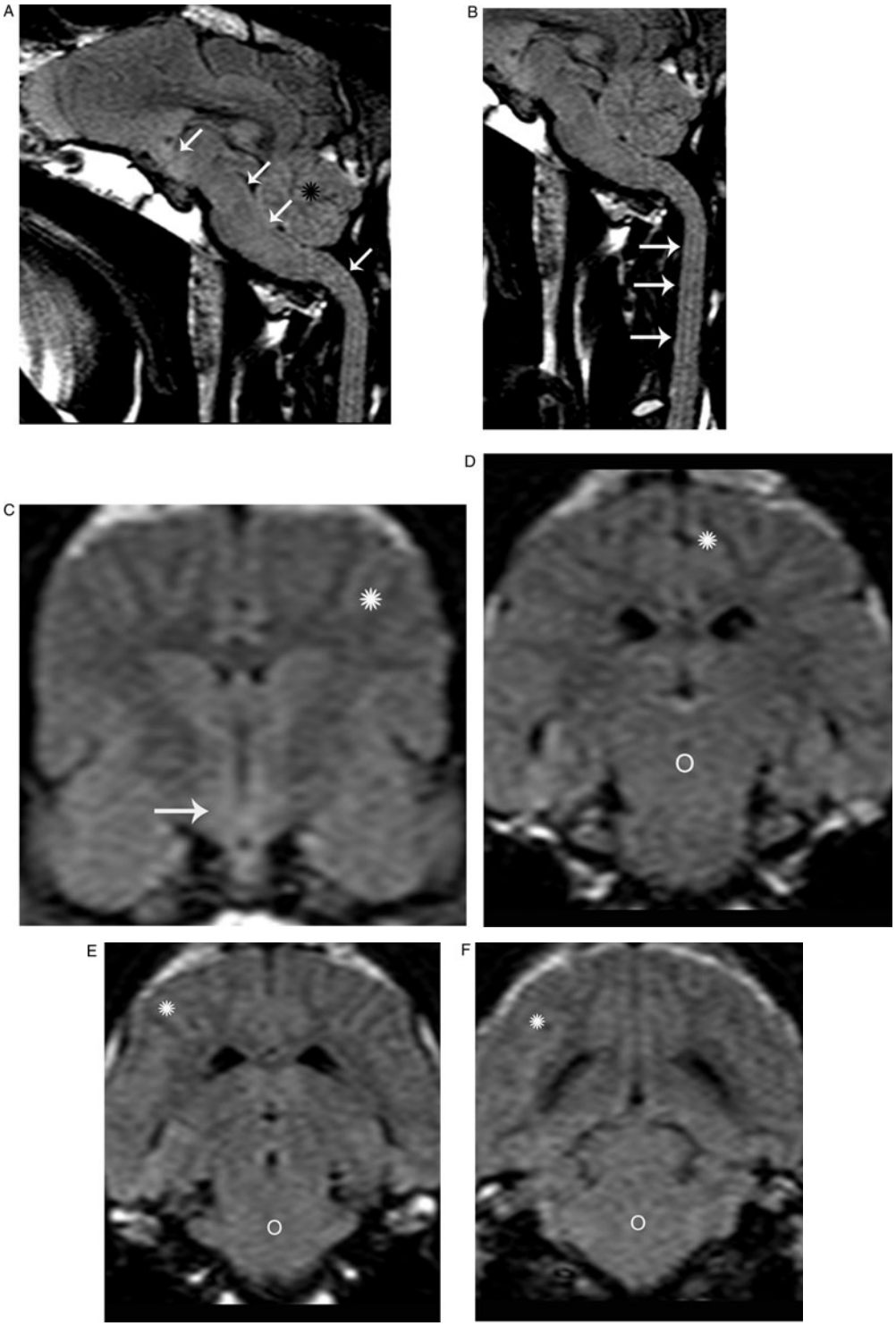


**Figure 2** Sagittal and coronal T2-weighted FLAIR MR images of a furious rabid dog brain reveal more diffuse mild to moderate hypersignal T2 changes involving hypothalamus, thalamus, midbrain, pons, medulla and spinal cord (*white arrows* in A to C and *white circles* in D toF), and hippocampi. Changes also involve the cerebrum (white asterix in C to F) and infratentorial cerebellum (black asterix in A).

The numbers of dogs studied were limited because naturally infected dogs were chosen. This would simulate what we encounter in humans. There are major barriers to using dogs in experiments in Buddhist countries such as Thailand. An experimental design having dogs inoculated with different virus dosages might give more control over when and how they were infected. Nevertheless, we have previously shown that sites of a bite did not influence the clinical expression of furious or paralytic

rabies (Tirawatnpong *et al*, 1989). We chose to define stage of disease as clinical stage (early or late) rather than the interval between time of exposure and examination because this actually reflects the functional status of the nervous system of the infected individual (Hemachudha, 1989). The virus may remain latent at the exposure site and the incubation period can be variable (Hemachudha and Phuapradit, 1997; Hemachudha *et al*, 2006). We studied only a small number of late-stage dogs, though they were easier to find, because we focused mainly on what actually happened during the early stage.

Our present data suggest that timing of MRI examination is critical. This might explain why both furious and paralytic rabies patients in our previous study had similar MRI patterns (Laothamatas *et al*, 2003). Localization of MRI abnormalities in rabid dogs did not correlate with loci that might be related to furious symptoms.

IFN-$\gamma$ as well as IL-1$\beta$ were present only in the brains of paralytic dogs. This suggests that the capacity to respond to rabies infection in paralytic dogs may be greater compared to their furious counterparts. IFN-$\gamma$ has been shown to be produced by migratory T cells invading the brains of mice infected with attenuated Pasteur strain rabies virus (Galelli *et al*, 2000). These mice recovered with or without paralytic sequele. Increased production in IL-1$\alpha$ and diminished binding sites have been shown in rabies-infected mouse brain, particularly in the hippocampus (Marquette *et al*, 1996a). Proinflammatory cytokines, such as IL-1$\beta$, in rabies-infected rat brains could be produced by resident microglia and infiltrating macrophages (Marquette *et al*, 1996b). Therefore, it is possible that there might be cells that have crossed the blood-brain barrier (BBB) at certain stages in paralytic rabies, which may be associated with some degree of leakage (Roy *et al*, 2007). In an animal model, virus pathogenicity also inversely correlates with the number of T cells migrating into the rabies-infected brains (Baloul *et al*, 2004; Roy *et al*, 2007; Wang *et al*, 2005).

We failed to demonstrate evidence of BBB leakage by MRI during the early stage of human rabies patients (Laothamatas *et al*, 2003) and rabies-infected dogs (in this study). No gadolinium-enhanced lesions were evident. Rabies-neutralizing antibody could not be detected in the CSF of a furious rabies patient who had received very high doses of intravenous human rabies immune globulin (Hemachudha *et al*, 2003a). Furthermore, cellular infiltrates were scant in the cerebral hemispheres of our rabies-infected dogs (data not shown) and in human rabies patients of both forms (Hemachudha *et al*, 2006; Juntrakul *et al*, 2005; Tirawatnpong *et al*, 1989). The degree of cellular infiltration in the brainstem of rabies-infected dogs and humans was variable and did not correlate with clinical manifestations. Marked cellular infiltration was found only in the peripheral nerves of paralytic rabies patients (Hemachudha *et al*, 2005; Mitrabhakdi *et al*, 2005). Lack of cellular infiltration in the cerebral hemisphere of rabies-infected humans and dogs may be explained by destruction of T cells that invade the CNS via increasing immunosubversive molecules, such as FasL (Baloul and Lafon, 2003; Lafon, 2004). We are intrigued by our findings that paralytic rabies-infected dogs have higher cytokine expression in the brains than furious dogs.

Our data suggest that a stronger CNS and perhaps earlier inflammatory response resulting in a delayed spread of infection may explain the longer survival in paralytic rabies. Moreover, this does not support the role of immune accelerated death in explaining the rapid fatal course in furious rabies. The dog may be a promising model to further study the relationship between virus and inflammatory responses in the brain.

## Materials and methods

*Animals*

A total of 13 dogs were used. Three were normal controls and 10 were proven rabies infected. All, except one control that was injured by a car and included in the virus and cytokine studies, were community dogs abandoned after they were bitten by suspected rabid dogs. None had been previously vaccinated. Each was observed for rabies symptoms at the quarantine and diagnostic unit of the Queen Saovabha Memorial Institute (QSMI). Sites of bites were mainly the head and face. After symptoms suggestive of rabies developed, the diagnosis was confirmed by demonstration of rabies viral RNA in saliva by nucleic acid sequence–based amplification (NASBA) (Wacharapluesadee and Hemachudha, 2001). Results were known within 3 to 4 h.

Categorization of furious or paralytic rabies was based on the following: aggression and biting behavior in dogs was associated with the former, and hind limb paresis with none or only a mild degree of aggression in dogs with the latter type (Tepsumethanon *et al*, 2005). The term "stage of infection" was clinically defined as early or late, based on whether the dogs remained fully conscious (early) or lapsed into coma (late) as previously described (Tirawatnpong *et al*, 1989). After the diagnosis was confirmed, these dogs were transferred for MRI at the Neuroimaging Center, Ramathibodi Hospital. All were in the early stage and remained conscious. Examination was done within 48 h, usually 24 h, after onset of the first clinical symptoms.

Two paralytic, two furious, and two uninfected dogs were included in the MRI study. During transfer and examination, the dogs were sedated with ketamine and pentobarbitone sodium. All rabies-infected dogs were humanely sacrificed at the completion of examination. Eight (four furious and four paralytic) rabies-infected dogs during the early stage

were included in the viral load study. Four (two furious and two paralytic) of them were also included in the cytokine study. Additionally, we studied one furious and one paralytic dog in the late stage for viral load and cytokines. The control dog, injured by a car, was also included.

The studies were approved by the research and ethics committee of Ramathibodi Hospital.

*MRI examination*

Studies were performed with a 3-tesla superconductive magnet (Intera; Philips Medical System, Best, The Netherlands). MR imaging of the brain and upper spinal cord was performed with SENSE Flex-M coils ( Philips Medical System) in axial and coronal diffusion-weighted image (DWI; TR/TE/ EPI/FOV: 2568/88/47/160; b-value of 0 and 1000 s/mm$^2$), sagittal and coronal T2-weighted fluid-attenuated inversion recovery (FLAIR) (TR/TE/TI/ET/matrix: 11,000/120/280/30/256 × 180), and T1-weighted (TR/TE/matrix: 500/11/256 × 200) before and after gadolinium administration, 0.1 mmol/kg, (Magnevist, Schering, Germany).

*Collection of samples for viral load and cytokine studies*

Brain specimens were collected from 12 anatomical locations at brainstem (midbrain, pons and medulla), thalamus, basal ganglia (putamen and globus palludus), caudate nucleus, temporal cortex, hippocampus (including CA1–4 regions), cortices of frontal, parietal and occipital regions, and cerebellum (mainly at the vermis). The diagnosis of rabies was confirmed by the presence of rabies antigen and viral N RNA in the brain by direct fluorescent antibody test and NASBA. All brains were kept under −80°C until examination.

*Extraction of RNA and reverse transcription*

Total RNA was extracted using the RNeasy Lipid Tissue Mini Kit (Qiagen, Hilden, Germany). Brain tissue was homogenized in 1 ml of QIAzol Lysis Reagent (Qiagen). The sample was vortexed and 200 $\mu$l of chloroform was added. The sample was incubated at room temperature for 10 min then centrifuged at 12,000 × *g* for 15 min at 4°C. RNA contained in the aqueous phase was transferred to a new tube and processed according to instructions from the manufacturer (Qiagen). The residual DNA was removed by the column DNase-digestion method using the RNase-Free DNaseSet (Qiagen). Total RNA was quantified using a SmartSpec 3000 Spectrometer (BioRad, Hercules, USA). First-strand cDNA synthesis was carried out with 1 $\mu$g of total RNA using the supplied random primer in 20 $\mu$l total volume under the following conditions: 70°C for 5 min for random primer annealing, 5 min on ice, annealing at 25°C for 5 min, first-strand synthesis at 42°C for 60 min, and inactivation at 70°C for 15 min (Improm-II reverse transcription system; Promega, Madison, WI, USA). cDNA concentrations were adjusted with RNase and DNase free water to 25 and 2.5 ng/$\mu$l for cytokine and viral quantitation assays, respectively.

*Rabies virus quantification by TaqMan real-time PCR*

Rabies viral load was measured by a real-time polymerase chain reaction (PCR) assay. The primer set for the rabies N gene was 5′-CTGGCAGACGACGGAACC-3′and 5′-CATGATTCG-AGTATAGACAGCC-3′. The Taqman fluorescent probe was 5′-FAM-TCAATTCTGATGACGAGGAT TACTTCTCCGG-TAMRA-3′. Five nanograms of sample cDNA were added to a 20-$\mu$l reaction volume of PCR mixture containing 1× Taqman PCR master mix (QuantiTect Probe PCR, Qiagen), 500 nM of each primer, and 200 nM probe. Thermal cycler conditions were 15 min at 95°C, and 45 cycles of 5 s at 95°C, followed by 1 min at 60°C. Dilutions of cDNA of single antisense-stranded rabies RNA obtained from T7 *in vitro* transcription (Riboprobe *in vitro* transcription systems; Promega) were used to prepare a standard curve. All standards and samples were assayed in the Light Cycler instrument (Roche Molecular Systems, Indianapolis, IN). The rabies viral load was calculated by the following formula: copy number of rabies per $\mu$g total RNA = (copy number per $\mu$l)/(total RNA concentration per $\mu$l). Each reaction included a negative control (water). The positive control included known amounts of synthetic rabies RNA.

*Semiquantification of cytokine mRNA*

PCR was performed on the reversely transcribed (RT) cDNA product to determine the expression of mRNA encoding cyclooxygenase (COX)-2, FGF, GM-CSF, IFN-$\gamma$, IL-1$\beta$, IL-2, IL-4, IL-5, IL-6, IL-8, IL-10, IL-12 p35, IL-12 p40, IL-18, MCP-1, TLR-4, TNF-$\alpha$, TGF-$\beta$, and vascular endothelial growth factor (VEGF)-164, -188, and -206 (Canine Primer Sets; Endogen, Pierce, Rockford, IL) according to the manufacturer's instructions. Normalization of the samples was accomplished using RT-PCR of the housekeeping gene GAPDH (Chamizo *et al*, 2005) to control the efficacy of the RNA extraction, its integrity, and the amount of RNA present. Controls were incorporated in each set of PCR reactions. Positive control included the synthetic DNA with different product size supplied by the manufacturer. Negative control included "no RNA" (water). Conditions for the PCR were as follows: after initial denaturation at 95°C for 2 min, 35 amplification cycles were conducted in a DNA thermocycler (model 9600, Perkin Elmer). Each cycle consisted of denaturation at 95°C for 30 s, annealing at 55°C for 30 s, and extension at 72°C for 1 min. PCR components included PCR buffer (1×; Promega), $MgCl_2$ (2.0 mM; Promega), dNTP mix (0.2 mM; Invitrogen), Taq DNA polymerase (2.5 U; Promega), 2 $\mu$l of the Primer Set solution (Pierce), and 2 $\mu$l of sample cDNA (25 $\mu$g/$\mu$l)

or 1 $\mu$l of the positive control in a 50-$\mu$l reaction volume.

Ten microliters of the amplified product were analyzed by agarose gel electrophoresis (2% agarose, containing 0.3 $\mu$g/$\mu$l ethidium bromide) and subsequently visualized and documented on a Gel Doc 2000 system (BioRad, Hercules, USA). The cytokines and GAPDH RT-PCR products of each RNA sample from 12 brain regions of the same dog were run in parallel. In order to quantify the intensity of the ethidium bromide signals, the gel was scanned with standard video imaging equipment and the images were analyzed with an image analysis software package with an integrated density program (Multi-analyst TM /PC version 1.1. BioRad, USA). The software graphically represented the bands of DNA present in each lane of the gel, calculating the value of the corresponding area. The cytokine expression rates were calculated as a ratio of cytokine to GAPDH area from the same sample (Chamizo et al, 2005). A ratio of >1 was considered significant.

## References

Baloul L, Camelo S, Lafon M (2004). Up-regulation of Fas ligand (FasL) in the central nervous system: a mechanism of immune evasion by rabies virus. *J NeuroVirol* **10:** 372–382.

Baloul L, Lafon M (2003). Apoptosis and rabies virus neuroinvasion. *Biochimie* **85:** 777–88.

Chamizo C, Moreno J, Alvar J (2005). Semi-quantitative analysis of cytokine expression in asymptomatic canine leishmaniasis. *Vet Immunol Immunopathol* **103:** 67–75.

Denduangboripant J, Wacharapluesadee S, Lumlertdacha B, Ruankaew N, Hoonsuwan W, Puanghat A, Hemachudha T (2005). Transmission dynamics of rabies virus in Thailand: implications for disease control. *BMC Infect Dis* **5:** 52.

Galelli A, Baloul L, Lafon M (2000). Abortive rabies virus central nervous infection is controlled by T lymphocyte local recruitment and induction of apoptosis. *J NeuroVirol* **6:** 359–372.

Hemachudha T (1989). Rabies. In: *Handbook of clinical neurology viral disease*. Vinken P, Bruyn G, Klawans H (eds). Elsevier Science Publishers: Amsterdam, pp 383–404.

Hemachudha T (1994). Human rabies: clinical aspects, pathogenesis, and potential therapy. *Curr Top Microbiol Immunol* **187:** 121–143.

Hemachudha T, Laothamatas J, Rupprecht CE (2002). Human rabies: a disease of complex neuropathogenetic mechanisms and diagnostic challenges. *Lancet Neurol* **1:** 101–109.

Hemachudha T, Panpanich T, Phanuphak P, Manatsathit S, Wilde H (1993). Immune activation in human rabies. *Trans R Soc Trop Med Hyg* **87:** 106–108.

Hemachudha T, Phanuphak P, Sriwanthana B, Manutsathit S, Phanthumchinda K, Siriprasomsup W, Ukachoke C, Rasameechan S, Kaoroptham S (1988). Immunologic study of human encephalitic and paralytic rabies. Preliminary report of 16 patients. *Am J Med* **84:** 673–677.

Hemachudha T, Phuapradit P (1997). Rabies. *Curr Opin Neurol* **10:** 260–267.

Hemachudha T, Sunsaneewitayakul B, Mitrabhakdi E, Suankratay C, Laothamathas J, Wacharapluesadee S, Khawplod P, Wilde H (2003a). Paralytic complications following intravenous rabies immune globulin treatment in a patient with furious rabies. *Int J Infect Dis* **7:** 76–77.

Hemachudha T, Wacharapluesadee S, Laothamatas J, Wilde H (2006). Rabies. *Curr Neurol Neurosci Rep* **6:** 460–468.

Hemachudha T, Wacharapluesadee S, Lumlertdaecha B, Orciari LA, Rupprecht CE, La-Ongpant M, Juntrakul S, Denduangboripant J (2003b). Sequence analysis of rabies virus in humans exhibiting encephalitic or paralytic rabies. *J Infect Dis* **188:** 960–966.

Hemachudha T, Wacharapluesadee S, Mitrabhakdi E, Wilde H, Morimoto K, Lewis RA (2005). Pathophysiology of human paralytic rabies. *J NeuroVirol* **11:** 93–100.

Juntrakul S, Ruangvejvorachai P, Shuangshoti S, Wacharapluesadee S, Hemachudha T (2005). Mechanisms of escape phenomenon of spinal cord and brainstem in human rabies. *BMC Infect Dis* **5:** 104.

Kalita J, Misra UK, Pandey S, Dhole TN (2003). A comparison of clinical and radiological findings in adults and children with Japanese encephalitis. *Arch Neurol* **60:** 1760–1764.

Khawplod P, Shoji Y, Ubol S, Mitmoonpitak C, Wilde H, Nishizono A, Kurane I, Morimoto K (2006). Genetic analysis of dog rabies viruses circulating in Bangkok. *Infect Genet Evol* **6:** 235–240.

Lafon M (2004). Subversive neuroinvasive strategy of rabies virus. *Arch Virol Suppl***:** 149–159.

Laothamatas J, Hemachudha T, Mitrabhakdi E, Wannakrairot P, Tulayadaechanont S (2003). MR imaging in human rabies. *AJNR Am J Neuroradiol* **24:** 1102–1109.

Lumlertdacha B, Boongird K, Wanghongsa S, Wacharapluesadee S, Chanhome L, Khawplod P, Hemachudha T, Kuzmin I, Rupprecht CE (2005). Survey for bat lyssaviruses, Thailand. *Emerg Infect Dis* **11:** 232–236.

Lumlertdacha B, Wacharapluesadee S, Denduangboripant J, Ruankaew N, Hoonsuwan W, Puanghat A, Sakarasaeranee P, Briggs D, Hemachudha T (2006). Complex genetic structure of the rabies virus in Bangkok and its surrounding provinces, Thailand: implications for canine rabies control. *Trans R Soc Trop Med Hyg* **100:** 276–281.

Marquette C, Ceccaldi PE, Ban E, Weber P, Tsiang H, Haour F (1996a). Alteration of interleukin-1 alpha production and interleukin-1 alpha binding sites in mouse brain during rabies infection. *Arch Virol* **141:** 573–585.

Marquette C, Van Dam AM, Ceccaldi PE, Weber P, Haour F, Tsiang H (1996b). Induction of immunoreactive interleukin-1 beta and tumor necrosis factor-alpha in the brains of rabies virus infected rats. *J Neuroimmunol* **68:** 45–51.

Mitrabhakdi E, Shuangshoti S, Wannakrairot P, Lewis RA, Susuki K, Laothamatas J, Hemachudha T (2005). Difference in neuropathogenetic mechanisms in human furious and paralytic rabies. *J Neurol Sci* **238:** 3–10.

Pleasure SJ, Fischbein NJ (2000). Correlation of clinical and neuroimaging findings in a case of rabies encephalitis. *Arch Neurol* **57:** 1765–1769.

Roy A, Phares TW, Koprowski H, Hooper DC (2007). Failure to open the blood-brain barrier and deliver immune effectors to central nervous system tissues leads to the lethal outcome of silver-haired bat rabies virus infection. *J Virol* **81:** 1110–1118.

Sheikh KA, Ramos-Alvarez M, Jackson AC, Li CY, Asbury AK, Griffin JW (2005). Overlap of pathology in paralytic rabies and axonal Guillain-Barre syndrome. *Ann Neurol* **57:** 768–772.

Tepsumethanon V, Wilde H, Meslin FX (2005). Six criteria for rabies diagnosis in living dogs. *J Med Assoc Thai* **88:** 419–422.

Tirawatnpong S, Hemachudha T, Manutsathit S, Shuangshoti S, Phanthumchinda K, Phanuphak P (1989). Regional distribution of rabies viral antigen in central nervous system of human encephalitic and paralytic rabies. *J Neurol Sci* **92:** 91–99.

Wacharapluesadee S, Hemachudha T (2001). Nucleic-acid sequence based amplification in the rapid diagnosis of rabies. *Lancet* **358:** 892–893.

Wang ZW, Sarmento L, Wang Y, Li XQ, Dhingra V, Tseggai T, Jiang B, Fu ZF (2005). Attenuated rabies virus activates, while pathogenic rabies virus evades, the host innate immune responses in the central nervous system. *J Virol* **79:** 12554–12565.